Int. J. Electron. Commun. (AEÜ) 138 (2021) 153873

Contents lists available at ScienceDirect

International Journal of Electronics and Communications

journal homepage: www.elsevier.com/locate/aeue

Regular paper

An improved analytical model for broadside coupled transmission line used on planar circuit

Renbin Tong [a,*], Jörgen Olsson [b], Dragos Dancila [a]

[a] Division of Solid-State Electronics, Department of Electrical Engineering, Ångström Labratory, Uppsala University, P.O. Box 65, SE-75103 Uppsala, Sweden
[b] Department of Materials Science and Engineering, Ångström Labratory, Uppsala University, 75103 Uppsala, Sweden

ARTICLE INFO

Keywords:
Analytical model
Broadside coupled line
Coplanar waveguide

ABSTRACT

Broadside coupled transmission lines have the advantage of more compact size and higher coupling factor compared to the traditional coupled microstrips in the realization of planar circuits such as substrate integrated baluns, directional couplers, and filters on printed circuit boards. A broadside coupled transmission line is a structure with interesting properties composed of two signal lines with strong coupling placed on the top and bottom of a dielectric substrate, surrounded by coplanar ground. This configuration allows the realization of the practical circuit with several hundred ohms impedance for even mode excitation, with the help of lower even mode capacitance. This leads to a high coupling factor and benefits to a high impedance transformation ratio balun or a wide bandwidth filter design. In this paper, an analytical model describing the symmetrical pair of conductors for broadside coupled transmission lines is presented. The analytical model based on the physical geometries of the coupled lines is verified by electromagnetic (EM) simulations and measurements. The results are in very good agreement with each other.

1. Introduction

When two unshielded transmission lines are in close proximity, power can be coupled from one line to the other due to the interaction of electromagnetic fields. The power can be coupled from one line to the other due to the interaction of electromagnetic fields. Such lines are called coupled transmission lines [1]. Coupled transmission lines can support two distinct propagating modes, and this feature can be used to implement a variety of practical directional couplers, hybrids, and filters. Generally, coupled transmission lines can be implemented with microstrip, stripline, or even coaxial lines.

The cross-sectional view of the well-studied traditional coupled microstrip line is illustrated in Fig. 1(a). The two signal lines are located on the same side, i.e., the top side, while the ground plane (GND) is located on the opposite side. The electrical characteristics of such coupled microstrip lines can be completely determined from the effective capacitances between the lines. The related formula analysis is fully investigated in [1]. Such structure is successfully used in filter and power divider design [2–6], etc. Moreover, [7] presents a method to estimate the near-end and far-end cross-talk of a coupled transmission lines based on eigenvector decomposition. While the cross-sectional view of the broadside coupled transmission line is depicted in Fig. 1 (b). It can be seen as two coplanar waveguides (CPWs) transmission lines [8] mounted back-to-back, without ground combined together. It can also be seen as a broadside coupled stripe line [8] without cover but with the suspended ground. Due to its simplicity and compactness, this structure can easily be realized on printed circuit boards (PCB).

In practical applications, such as for wider bandwidth filters, balun with high impedance transformation ratio, etc. They generally require very tightly coupled lines to pursue the high coupling factor, which is difficult to fabricate for the traditional coupled microstrip lines. But this feature can be easily implemented by broadside coupled lines because of its relatively smaller equivalent capacitance under even-mode excitation. This broadside coupled structure is successfully used for the design of planar balun as output matching network in [9,10]. However, to the best of the author's knowledge, the circuit design based on this structure completely relies on EM simulations, and there is no systematic investigation of this structure and no analytic model yet for the designer to refer to as to guide for engineering the coupled lines [11–13]. Therefore, such a model is developed in this paper using the same methods as for coplanar waveguides [14] and adapting the model for broadside coupled transmission lines to extract the even and odd characteristic

* Corresponding author.
E-mail address: renbin.tong@angstrom.uu.se (R. Tong).

https://doi.org/10.1016/j.aeue.2021.153873
Received 6 April 2021; Accepted 18 June 2021
Available online 24 June 2021

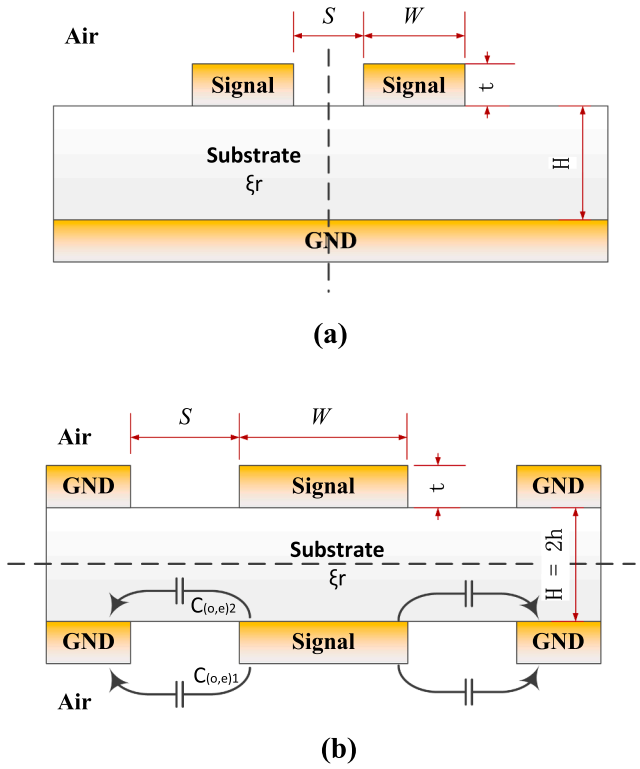

Fig. 1. Cross-sectional view of (a) conventional coupled micrstrip line; and (b) broadside coupled transmission line. Where the dashed line represents the E-wall or H-wall.

impedances. Analytical formula derivation based on the even and odd impedance analysis is presented in Section 2. Section 3 presents a comparison among EM simulations using the commercial software ANSYS Electronics HFSS and measurements is adopted to verify the derived analytical model. Very good agreements are obtained.

2. Theoretical analysis

The configuration under investigation is sketched in Fig. 1(b). It is a structure composed of two signal traces (Signal) placed on top and bottom of a dielectric substrate, surrounded by ground and realizing a microwave coupled transmission line. The height of the dielectric substrate is H, and the relative dielectric constant is $\in_r$. The signal trace is located on the middle of two separated ground traces (GND). The distance or gap between Signal and GND is defined as S, and the width of the signal trace is defined as W. Generally, for PCB applications, the signal and ground trace is copper, and the thickness t is normally 1 oz (1.35 mil), for simplicity, the copper thickness was ignored in the following analytical derivation.

In this paper, start with the analytical model based on coplanar waveguide [8] and broadside coupled stripline [15] to calculate the $C_{(o,e)2}$ in dielectric layer that depicted in Fig. 1(b). Then improved formulas for $C_{(o,e)1}$ are derived to applied to the air layer with infinity height. Importantly, a coefficient $\alpha_{(o,e)}$ is employed to correct the $C_{(o,e)1}$ since the changed boundary conditions. Additionally, to simplify the analytical process, separate the structure into two symmetrical planes by a magnetic wall or electric wall with even-mode or odd-mode excitation.

Based on this strategy, the characteristic impedance derivations are derived as follows.

2.1. Even mode

Follow the general idea to formulate even/odd mode characteristic impedance, the analytic expression for even/odd mode characteristic impedance is given by:

$$Z_{0e} = \left[c_v\sqrt{C_e C_e^a}\right]^{-1} \tag{1}$$

where c_v is the velocity of propagation in free space, c_v=2.998 × $10^8 m/s$. C_e is the even-mode capacitance per unit length, C_e^a is the capacitance when the substrate's dielectric is replaced by air. To express the C_e effectively, the structure in Fig. 1 can be modeled as two symmetrical half-planes which are separated by magnetic walls (dashed line in Fig. 1, its corresponding E field distribution is illustrated in Fig. 2(a)). Due to the symmetrical distribution of the E field, the total even-mode capacitance C_e can be considered as the sum of two components, C_{e1} and C_{e2}, representing the capacitance in air and dielectric, respectively. Then the equations with physical dimensions can be written as follows:

$$C_e = C_{e1} + C_{e2} \tag{2}$$

k_{e1} and k_{e2} are two intermediate parameters involved in the derivation of the two capacitors above. Observably, k_{e1} is the case of k_{e2} when the height h goes to infinity high. To be accurate, a coefficient α_e is employed to illustrate the fact that no cover and suspended ground in the air layer. They are expressed as follows:

$$k_{e1} = \frac{W}{W+2S} \tag{3}$$

$$k_{e2} = \sinh\left(\frac{\pi W}{4h}\right) \Big/ \sinh\left(\frac{\pi(W+2S)}{4h}\right) \tag{4}$$

$$C_{e1} = 2\alpha_e \in_0 \frac{K(k_{e1})}{K(k_{e1}^{'})} \tag{5}$$

$$C_{e2} = 2\in_0 \in_r \frac{K(k_{e2})}{K(k_{e2}^{'})} \tag{6}$$

where $K(k)$ and $K(k^{'})$ are the complete elliptic integrals of the first kind

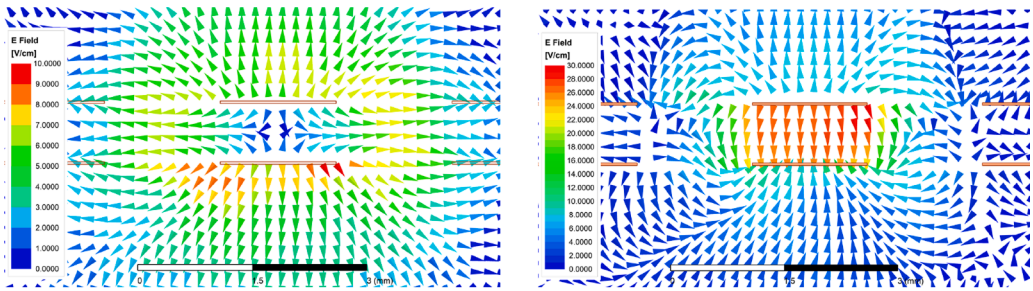

(a) (b)

Fig. 2. Simulated vector E field graph for (a) even mode; (b) odd mode.

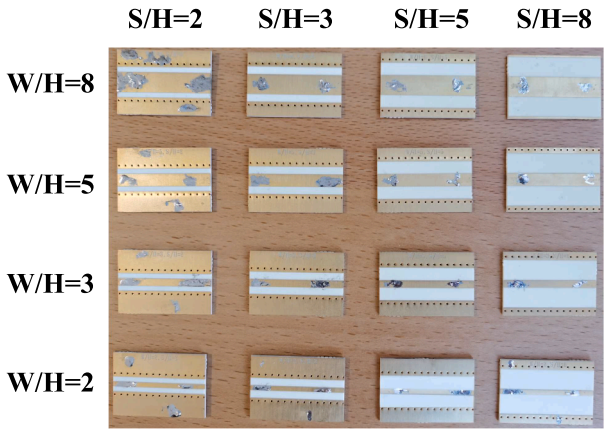

Fig. 3. Fabricated designs with different dimensions. The layout at the top and the bottom side are symmetrical same. They will be used as DUT in measurement. All DUT has the same length 28.8 mm.

and their complements, and $k' = \sqrt{1-k^2}$. A third degree polynomials (cubic polynomials) function is involved to describe α_e, and similarly to α_o that under the odd mode excitation. The expression can be written as $\alpha_e = c_0 + a_1x + a_2x^2 + a_3x^3 + b_1y + c_1xy + c_2x^2y$, where $x = W/H$, and $y = S/H$.

For the even mode, based on the simulated and measured results, all coefficients are derived as follows: $c_0 = 2.518$, $a_1 = -0.9556$, $a_2 = 0.2631$, $a_3 = -0.01964$, $b_1 = 0.008868$, $c_1 = -0.01533$, $c_2 = 0.00146$.

2.2. Odd mode

A same analysis process with even mode, but take the magnetic wall under even mode as the electrical wall under odd mode in Fig. 1(b). Its corresponding E field distribution is illustrated in Fig. 2(b). Then the total capacitance of odd mode can be described as $C_o = C_{o1} + C_{o2}$, then all equations are given by:

$$Z_{0o} = \left[c_v\sqrt{C_oC_o^a}\right]^{-1} \tag{7}$$

$$k_{o1} = \frac{W}{W+2S} \tag{8}$$

$$k_{o2} = \tanh\left(\frac{\pi W}{4h}\right)\Big/\tanh\left(\frac{\pi(W+2S)}{4h}\right) \tag{9}$$

$$C_{o1} = 2\alpha_o\in_0\frac{K(k_{o1})}{K(k'_{o1})} \tag{10}$$

$$C_{o2} = 2\in_0\in_r\frac{K(k_{o2})}{K(k'_{o2})} \tag{11}$$

Similar with α_e, α_o is updated as $\alpha_o = c_0 + a_1x + a_2x^2 + b_1y + b_2y^2 + c_1xy$.

For the odd mode, the coefficients of α_o based on simulated and measured results is derived as: $c_0 = 3.338$, $a_1 = 0.9781$, $a_2 = -0.01318$, $b_1 = -0.1021$, $b_2 = -0.04674$, $c_1 = -0.1248$.

3. Analytical model verification

To verify the formulas derived in Section 2, coupled structures with different dimensions were simulated and fabricated. Practically, a matrix for W/H and S/H dimensions equal to 2, 3, 5 and 8 were fabricated on a commercial material: 30 mil Rogers 4350B with dielectric constant $\in_r = 3.66$. The responding fabricated circuits are shown in Fig. 3. The line length is 28.8 mm for all dimensions.

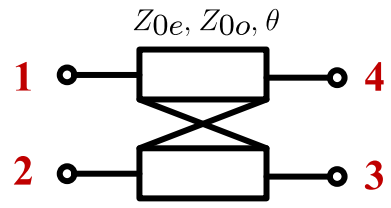

Fig. 4. Corresponding schematic model for the broadside coupled structure shown in Fig. 3 with specified port numbers.

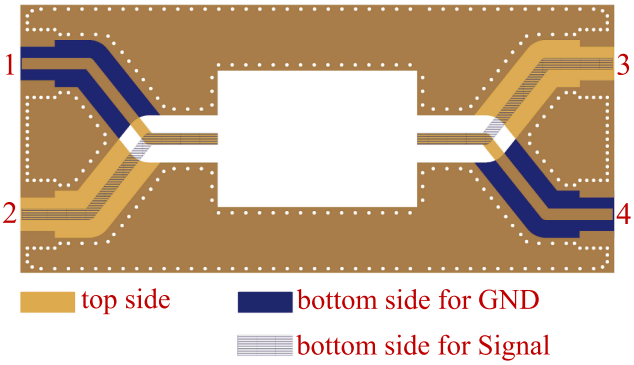

Fig. 5. The transparent layout for test fixture.

The corresponding schematic model with the specified port numbers is indicated in Fig. 4. The features of impedance matrix Z can be written as below for its symmetrical characteristic[1].

$$\begin{cases} Z_{11} = Z_{22} = Z_{33} = Z_{44} = \dfrac{-j}{2}(Z_{0e} + Z_{0o})\cot\theta \\ Z_{12} = Z_{21} = Z_{34} = Z_{43} = \dfrac{-j}{2}(Z_{0e} - Z_{0o})\cot\theta \\ Z_{13} = Z_{31} = Z_{24} = Z_{42} = \dfrac{-j}{2}(Z_{0e} - Z_{0o})\csc\theta \\ Z_{14} = Z_{41} = Z_{23} = Z_{32} = \dfrac{-j}{2}(Z_{0e} + Z_{0o})\csc\theta \end{cases} \tag{12}$$

where Z_{0e} and Z_{0o} are the even and odd impedance separately, θ is the electrical length.

Due to its symmetrical features, only Z_{11}, Z_{12}, Z_{13} and Z_{14} are

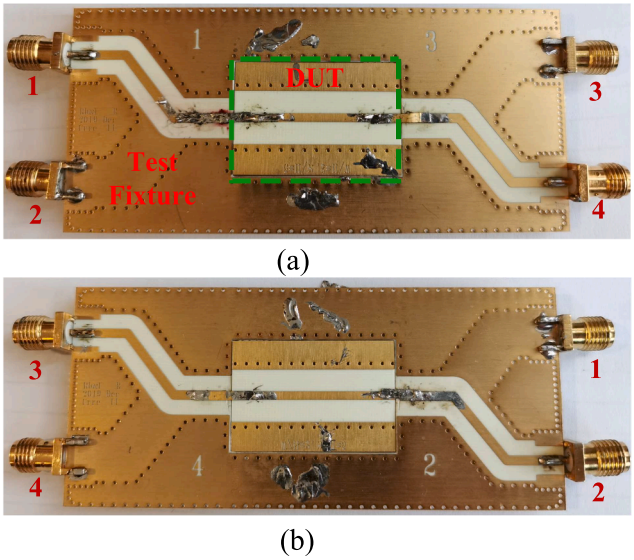

Fig. 6. Photograph of test fixture with DUT. (a) top side; (b) bottom side.

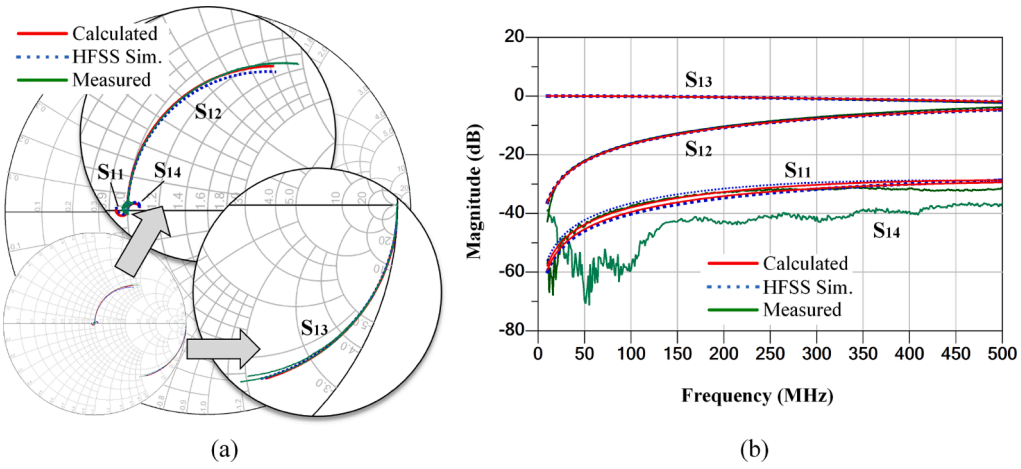

Fig. 7. Calculated, simulated and measured S-parameters for H = 30mil, S = 3 mm, W = 3 mm case in (a) Smith chart; (b) magnitude (dB).

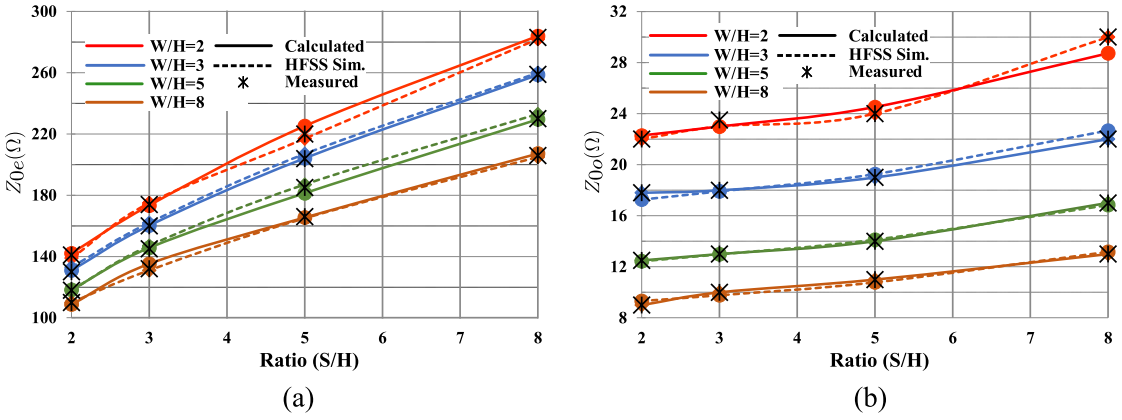

Fig. 8. Calculated, simulated and measured comparison results for (a) Z_{0e}; (b) Z_{0o}.

required to fully describe this structure. For simplicity, a factor k_f is introduced in this work, Z_{0e} and Z_{0o} then can be calculated as:

$$k_f = \sqrt{Z_{13}^2 - Z_{12}^2} \tag{13}$$

$$Z_{0e} = -j \times \left(k_f + k_f \frac{Z_{13}}{Z_{14}}\right) \tag{14}$$

$$Z_{0o} = j \times \left(k_f - k_f \frac{Z_{13}}{Z_{14}}\right) \tag{15}$$

In practise, the scattering matrix S is first simulated and measured, then convert them into Z matrix to calculate Z_{0e} and Z_{0o}.

For the S parameter measurements of these DUTs, for more clarity, the transparent layout of the test fixture without DUT shown in Fig. 5 was designed. Observably, two sides of PCB are used, which may increase little but not too much cost compared to conventional microstrip structure. While the photograph for the test fixture with DUT is shown in Fig. 6.

First, in measurements, the S-parameters of the whole board was measured, then de-embedding the test fixture to obtain the desirable broadside coupled line structure's S-parameters. The comparison of calculation, simulation and measurements of one special case when S = 3 mm and W = 3 mm are shown in Fig. 7. The calculated results matched well with simulations and measurements.

Finally, the calculated, simulated and measured characteristic impedances of the even and the odd modes are shown in Fig. 8(a) and Fig. 8 (b) respectively as a function of W/H and S/H. The analytical model match very well with the simulated and the measured results.

It can be observed that Z_{0o} is not sensitive with the gap space S between signal and ground trace that indicated in Fig. 8(a). This is also in agreement with predictions since the main capacitance of the even mode is from the parallel plate capacitor between the two signal traces. Meanwhile, it can be noticed that the even mode impedance Z_{0e} can reach up to more than 200 Ω, which means the coupling factor ($C_F = (Z_{0e} - Z_{0o})/(Z_{0e} + Z_{0o})$) is very high compared to the traditional coupled microstip structure.

4. Conclusions

Broadside coupled transmission lines are adequate to be used in planar baluns, directional couplers, and filters for their easy realization on PCB and have the advantage of compact features. This paper derives an analytical model that can be used to describe this complex structure as an aid in the design phase of other passive components based on these coupled transmission lines. Moreover, a method is introduced to calculate the even/odd characteristic impedance from measured scattering parameters. The analytical derivations are verified by EM simulations and measurements. The model shows very good agreement with the simulated and measured results for a large span of geometrical shapes of broadside coupled transmission line structures.

Declaration of Competing Interest

The authors declare that they have no known competing financial interests or personal relationships that could have appeared to influence the work reported in this paper.

Acknowledgments

The authors would like to thank the full support of the Eurostars programme: ENEFRF under E!11654 . And the authors are thankful for the continuous support and help of their colleagues in the FREIA Laboratory. The authors also appreciate Raul Timbus from ANSYS Inc. for his warm support on HFSS setup.

References

[1] Pozar DM. Microwave Engineering. John Wiley & Sons; 2009.
[2] Wang W, Zheng Y, Wu Y. A generalized broadband coupled-line based rat-race coupler with arbitrary power division ratios and free terminated impedances. AEU - Int J Electron Commun 2020;125:153388. https://doi.org/10.1016/j.aeue.2020.153388. URL https://www.sciencedirect.com/science/article/pii/S1434841120313571.
[3] Yildirim BS, Karayahsi K. Broadband UHF microstrip coupler. AEU - Int J Electron Commun 2019;108:91–5. https://doi.org/10.1016/j.aeue.2019.06.004. URL https://www.sciencedirect.com/science/article/pii/S1434841119305564.
[4] Sohi AK, Kaur A. Triple band-stop characteristics from an aperture coupled modified pythagorean tree fractal-based UWB-MIMO antenna integrated with complementary hexagonal spiral defected ground structure. AEU - Int J Electron Commun 2021;137:153805. https://doi.org/10.1016/j.aeue.2021.153805. URL https://www.sciencedirect.com/science/article/pii/S1434841121002028.
[5] Zhu H, Abbosh AM, Guo L. Wideband four-way filtering power divider with sharp selectivity and wide stopband using looped coupled-line structures. IEEE Microwave Wirel Compon Lett 2016;26(6):413–5. https://doi.org/10.1109/LMWC.2016.2562107.
[6] Zhang B, Wu Y, Liu Y. Wideband single-ended and differential bandpass filters based on terminated coupled line structures. IEEE Trans Microw Theory Tech 2017;65(3):761–74. https://doi.org/10.1109/TMTT.2016.2628741.
[7] Soleimani N, Alijani MG, Neshati MH. Crosstalk analysis at near-end and far-end of the coupled transmission lines based on eigenvector decomposition. AEU - Int J Electron Commun 2019;112:152944. https://doi.org/10.1016/j.aeue.2019.152944. URL https://www.sciencedirect.com/science/article/pii/S1434841119317157.
[8] Simons RN. Coplanar waveguide circuits, components, and systems, vol. 165. John Wiley & Sons; 2004.
[9] MRFX1K80H Datasheet, MRFX1K80H.pdf, [Online]. Available: https://www.nxp.com/docs/en/data-sheet/MRFX1K80H.pdf, Nov. 2018. URL https://www.nxp.com/docs/en/data-sheet/MRFX1K80H.pdf.
[10] Model MRF1K50-PLA FM pallet amplifier, MRF1K50-PLA.pdf, [Online]. Available: http://www.broadcastconcepts.com/80watt/MRF1K50-PLA.pdf, Nov. 2017. http://www.broadcastconcepts.com/80watt/MRF1K50-PLA.pdf.
[11] Dardeer OM, Elsadek HA, Elhennawy HM, Abdallah EA. Ultra-wideband bandstop filter with multiple transmission zeros using in-line coupled lines for 4G/5G mobile applications. AEU-Int J Electron Commun 2021;131:153635.
[12] Gong S, Xu X, Karlsson M. Broadside-coupled microstrip lines as low loss metamaterial for microwave circuit design. Wireless Commun Mobile Comput 2019.
[13] Xu X, Karlsson M, Gong S. Broadband and low-loss composite right/left-handed transmission line based on broadside-coupled lines. Int J RF Microwave Comput Aided Eng 2019;29(8):e21763.
[14] Ghione G, Naldi C. Parameters of coplanar waveguides with lower ground plane. Electron Lett 1983;19(18):734–5.
[15] Bedair SS, Wolff I. Fast and accurate analytic formulas for calculating the parameters of a general broadside-coupled coplanar waveguide for (M) MIC applications. IEEE Trans Microwave Theory Techn 1989;37(5):843–50.